The Abdus Salam
International Centre for Theoretical Physics

United Nations
Educational, Scientific and
Cultural Organization

IAEA
International Atomic Energy Agency

2055-10

Joint ICTP/IAEA School on Physics and Technology of Fast Reactors Systems

9 - 20 November 2009

Fast Reactor Core Design

Module 4 : Mechanical Design

P. Puthiyavinayagam
IGCAR
Kalpakkam
India

IAEA/ICTP School on Physics and Technology of Fast Reactor Systems

Lectures on Fast Reactor Core Design

Module 4 : Mechanical Design

Compiled & Delivered by

P,Puthiyavinayagam
IGCAR, Kalpakkam, India

The Abdus Salam
International Centre for Theoretical Physics
Trieste, Italy

Nov 9-20, 2009

CORE MECHANICAL DESIGN

4.0 INTRODUCTION

Subsequent to the thermal hydraulic aspects, core mechanical design becomes important which would again call for few iterations in the hydraulic design and also in relation with the material choice and its behaviour. The chief limiting factor for high burnup comes from SA bowing and dilation with the structural materials choices viz. austenitic stainless steels such as 316Ti, 316L, Ti stabilized steels etc. The ways and means of accommodating the bowing and dilation respecting the design criteria and design limits are given below. Also, mechanical design aspects governing the fuel pin such as fuel clad mechanical interaction, cumulative damage fraction approach and the optimum inter subassembly gap are dealt with.

The SA dilation should be accommodated either by going for advanced non-swelling material for the wrapper or by suitable design means. Design options are either to increase the inter SA gap or to increase the wrapper thickness. Either option influences the core volume fractions affecting the neutronics. Hence, the chosen dimensions of wrapper thickness and inter SA gap should be checked against neutronic parameter targets and optimum values are to be obtained in a few iterations.

One way is to design the core restraint in such a manner that the resultant SA deformations, interaction forces, SA extraction forces, reactivity changes due to bowing are within the limits prescribed. To obtain the desired targets, core restraint system should also be chosen in an appropriate manner. For example, while choosing the natural restraint system, the number of load pads and their locations should be chosen after detailed analysis. They should be sufficiently away from the high fluence zone.

Within a SA, once the dimensions of the wrapper, fuel pin diameter and spacer wire are finalized, it has to be analysed for possible bundle-wrapper interaction for fresh as well as target burnup conditions to check the porosity within the bundle. It is required to check for the coolant flow area reduction and hot channel temperature.

While the approach is expected to be similar in SA design, there would be design variants for which the methadology adopted will vary accordingly. In this notes, the design approach adopted is described in general terms with particular reference to PFBR.

4.1 FAILURE MECHANISMS

“Design by analysis” requires failure mechanisms to be clearly spelt out and the parameter to be reckoned for each failure mechanism. Following failure mechanisms are relevant:

1. Tensile instability due to membrane loading
2. Collapse in bending/possible cracking in outer fibres in bending
3. Ratchetting due to secondary stress cycling/possible cracking due to large secondary stress
4. Cracking at strain concentrations due to short-term loads (static notch weakening)
5. Creep rupture
6. Fatigue (this is not significant for core components)
7. Unstable crack propagation
8. Excessive deformation limited by functional requirements
9. Buckling (this is not significant for core components)

4.2 DESIGN SAFETY LIMITS

Design of components with sufficient margin is the first step in defence-in-depth principle adopted to ensure reactor safety. This requires consideration of all the loads in the components during normal operation as well as during off normal events. All the design basis events occurring during the lifetime of the components concerned are classified into four categories based on the frequency of occurrences. It is essential to define the design safety limits (DSL) for the four categories of events in order to assess that the design provisions of the system / components are adequate to ensure safety. The limits imposed are generally in terms of temperatures, radiation doses and structural design parameters. Limits are imposed on component / systems which could be broadly classified into three major groups. The first group comprises the core components whose performance conditions are vital for reactor safety and they form the primary barrier for the radioactive fission products. Second group comprises hot pool and cold pool systems and components with limits defined in terms of temperatures and structural parameters. This is the second barrier for the fission products in case of failure of first barrier i.e. clad. Third group comprises radiation limits to personals with respect to plant personnel, public at site boundary and public at neighbourhood. This lecture note discusses and summarizes the design safety limits derived for fuel, clad and coolant.

Philosophy of Limits Definition

For temperature limits concerning fuel, the criteria is to avoid fuel melting or limit the melting to as small a volume as possible. Hence, the limits for fuel are normally derived based on the extent of melting. Derivation of these limits in countries especially France and USA are based on fuel transient experiments undertaken.

For temperature limits concerning the clad, the criteria is to retain its integrity. The clad material is subjected to stresses and operating at high temperatures and hence undergo damage. The main damage is from creep considerations. Hence, for defining clad temperature limits, one suitable approach is to use Cumulative Damage Fraction (CDF) concept, for which structural design criteria for highly irradiated components and data on material behaviour under transients are very important. Since the limits are on the basis of damage, time duration also is to be defined for transients. Towards this, international experience and published literature data can be looked into.

For limits concerning the coolant, the philosophy is to avoid bulk coolant boiling or to limit the coolant boiling to the local spots. Hence, the limits for the coolant are normally derived based on coolant boiling. The limit to coolant boiling in local spots should be defined in such a way that it does not lead to systematic clad melting leading to material relocation.

4.3 DESIGN APPROACH

4.3.1 Types of analysis

Two types of analysis are usually followed – elastic & inelastic analysis. In the case of core components, because of neutron irradiation, elastic analysis may include swelling and irradiation induced creep which are not structurally damaging, but cause only deformation (similar to thermal strain, but irreversible). This type of analysis is called elastic/in pile creep/swelling analysis (EICSA). The limits followed for this type of analysis are same as that for elastic analysis.

The other type of analysis is the detailed inelastic analysis (IEA). While in EICSA the limits are on stresses, in the IEA the limits are on strains.

Design Rules

The relationship between protection against failure mechanisms and corresponding design rules for EICSA and for IEA are summarized in Tables 1 & 2.

In deciding the stress limits, especially for elastic analysis (the inelastic analysis is linked to strain limits), the ductility reduction under neutron dose requires careful considerations. In materials in which extensive strain hardening takes place (austenitic stainless steels which are used in core components) exceeding yield stress in a few special cases does not pose a problem because of capacity of large ductility to absorb moderate strains. In fact the rules for elevated temperature service allow for exceeding yield point in bending at outer fibres and also in case of secondary stresses in the shale-down regime. However, when the ductility becomes very low (approx. 1%), exceeding yield stress even at local points can be detrimental. In inelastic analysis, such limits can be explicitly defined. But in elastic analysis, such limits can be imposed only through stress limits and these are sought to be prescribed by linking with ductility of the material which is found to be well correlated with the ratio S_y/S_u of the irradiated material. The irradiated data in the case of ductility is shown in Fig.4.1. This may be used as a guideline when ductility value is not available and only S_y and S_u values are available.

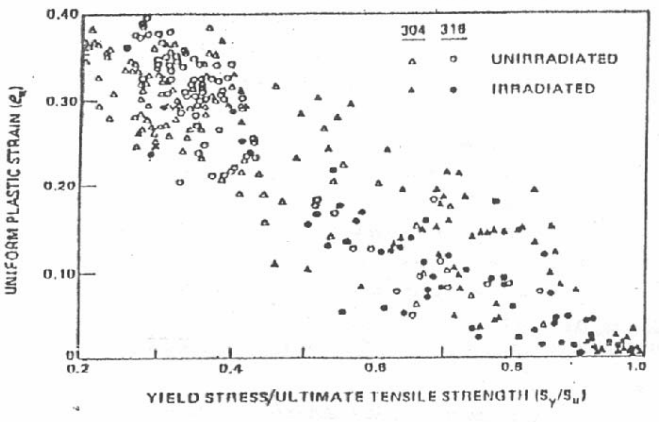

Fig. 4.1: Uniform Elongation Vs Ratio of Yield to Ultimate Tensile Strength

Stress Limits Approach

The stress limits to be satisfied for EICSA are given in Table-4.1. Two S_y/S_u thresholds have been considered in these limits. These are S_y/S_u = 0.7 beyond which the ductility of the irradiated material reduced below 5 % and S_y/S_u = 0.85 beyond which the ductility of the irradiated material reduced below 1 %. These ductility transitions are significant while considering limits in bending and for secondary stresses.

When the ductility is greater than 5 % (S_y/S_u < 0.7), the membrane stress limits, bending stress limits and secondary stress limits are all based on S_y. When the ductility is low, then these limits shall be based on S_u.

When ductility is very low, limits for bending loads (for ε_u < 5%) and for secondary stresses (for ε_u < 1%) are similar to those for membrane stresses. Higher stresses may be permitted for austenitic stainless steel when ductility is high, based on limit load approach and shake down mechanisms, respectively.

Strain Limits Approach

The strain limits to be satisfied for IEA are given in Table-4.2. To protect against plastic tensile instability due to loads which occur over the life of component, a summation rule is proposed as the ductility of the material varies depending on the neutron dose.

The limit on ε_m^p has been assumed as equal to ε_u / 2 which recommendation is based on experiments conducted on pressurized tubes.

Cumulative Damage Fraction (CDF) Approach

CDF uses a life fraction rule to find out the damage of the clad which includes damage happened in steady state operation and transient state. Tradiationally, CFD would include the creep and fatigue damage. But, in the case of fuel pin, the fatigue fraction will be insignificant and hence only creep is normally considered. Damage fraction at any particular interval of time is the ratio between the interval time and maximum time if subjected total damage would happen. If the damage fraction is integrated for the whole life of the clad gives the total damage of the clad. Cladding breach or rupture is implied by CDF of unity.

$$CDF = \int_0^t \frac{dt}{t_r(\sigma, T, \phi t)}$$

Where,

t_r - Time to rupture is maximum time if subjected to the given stress, temperature & fluence clad will operate without failure, h

σ -stress, MPa

T -temperature, K

Φt -fluence, n/cm^2

To find out the t_r, correlations are available in the literature for steady state as well as transient conditions. A typical correlation that can be used for D9 material to find out the t_r incase of steady state operation is given below:

$\log (t_r) = (5.4042 - \log(\sigma)) / (2.244 \times 10^{-4} T) - 13.5$

During reactor operation, different categories of events are envisaged. So, CDF is also apportioned for different category events as a design approach. In case of typical reactor like PFBR, the damage fraction under normal operation is limited to 0.25. A damage fraction of 0.5 is allotted for transient events, which cover category 2 and 3 events. Thus the remaining 0.25 is available for spent fuel storage and handling. Fig.4.2 shows the CDF for PFBR fuel pin as a function of burnup.

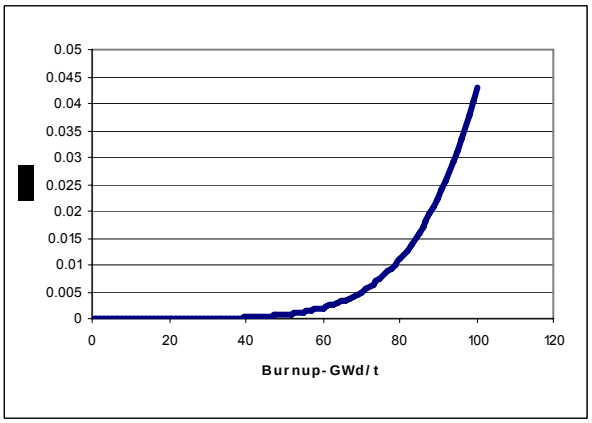

Fig. 4.2 : CDF Vs Burnup for typical fuel pin

Table 4.1: Failure Mechanisms & associated Design Rules for EICSA

Failure mode	Governing Parameter	Critical Value	Factor of Safety	Design Rule
Tensile instability	P_m	S_y or S_u	1.18 & 1.7 for cat. 1 &2 0.9 & 1.25 for cat. 3	P_m<0.85 S_y or < 0.6 S_u For category 1 & 2 loads P_m<1.1 S_y or < 0.8 S_u For category 3 loads
Failure in bending	P_m+ P_b	K $S_y$or S_u	Same as above	Same as above
Ratcheting	P_m+P_b+Q	Shake down limits or S_u	1.7 for cat. 1&2 and 1.25 for cat.3 on S_u	P_m+P_b+Q < 0.6 S_u For category 1 &2 P_m+P_b+Q < 0.8 S_u For category 3 loads
Localised rupture	P_m+P_b+Q+F	S_u	1.25 for cat. 1&2 and 1.1 for cat.3	P_m+P_b+Q+F< 0.8 S_u For cat. 1 &2 loads P_m+P_b+Q+F< 0.9 S_u For category 3
Damage due to creep & fatigue	Time duration , Δt and no. of cycles, n	Rupture life t_d and fatigue limit N	4 on CDF for cat. 1 , 2 for cat. 1 & 2 and 1.3 for cat. 1,2 &3	$\Sigma\Delta t/t_d$ + Σn/N < 0.25 for cat. 1 and < 0.5 for cat. 1 & 2 and < 0.75 for cat. 1,2 &3
Brittle fracture	K_I	K_{IC}	----	K_I < K_{IC}

Note : Factors of safety given for damage due to creep and fatigue are on cumulative damage fraction (CDF).

Table 4.2: Failure Mechanisms & associated Design Rules for IEA

Failure mode	Governing Parameter	Critical Value	Factor of Safety	Design Rule
Tensile instability & Ratcheting	ε_m^p	ε_u/2	3 for category 1 & 2 loads 1.5 for cat. 1,2 & 3	$\Sigma\varepsilon_m^p$/ (ε_u/2) <0.33 for cat. 1&2 $\Sigma\varepsilon_m^p$/ (ε_u/2) <0.66 for cat. 1,2 &3
Localised rupture	ε^p_t	ε_f/TF	2 for cat. 1 & 2 and 1.25 for cat. 1,2 &3	$\Sigma\varepsilon^p_t$/(ε_f/TF)<0.5 for cat. 1&2 $\Sigma\varepsilon^p_t$/(ε_f/TF)<0.8 for cat.1,2&3
Damage due to creep & fatigue	Time duration, Δt and no. of cycles, n	Rupture life t_d and fatigue limit N	4 on CDF for cat. 1 , 2 for cat. 1 & 2 and 1.3 for cat., 1,2 &3	$\Sigma\Delta t/t_d$ +Σ n/N < 0.25 for cat. 1 and < 0.5 for cat. 1 & 2 and < 0.75 for cat. 1,2 &3
Brittle fracture	J-integral	J_c	----	J < J_c

4.3.2 Design safety limits for a typical fast reactor

The design safety limits arrived at for a typical fast reactor, based on the approach described previously, are given below in table 4.3.

Table 4.3 : Typical Design Safety Limits
(All temperatures are in K, Time duration in Minutes)

<table>
<tr><td colspan="2" rowspan="2">PARAMETER</td><td colspan="4">EVENT CATEGORY</td></tr>
<tr><td>1</td><td>2</td><td>3</td><td>4</td></tr>
<tr><td colspan="2">FUEL HOTSPOT</td><td>No melting</td><td>No melting</td><td>No melting</td><td>50% fuel melting in max. rated pellet</td></tr>
<tr><td rowspan="3">CLAD HOTSPOT (temp in K)</td><td>Driver Fuel SA</td><td>973
and
CDF ≤ 0.25</td><td>974–1023 K for 75 m
and
1023-1073 K for 15 m
for all cate.2 events
and
CDF ≤ 0.25</td><td>974-1073 K for 15 m
and
1073–1123 K for 6 m
and
1123–1173 K for 2 m
and
CDF ≤ 0.25</td><td>1473</td></tr>
<tr><td rowspan="2">Storage SA</td><td>823</td><td>873</td><td>923</td><td rowspan="2">1223</td></tr>
<tr><td colspan="3">and CDF < 0.25</td></tr>
<tr><td colspan="2">AVERAGE SA COOLANT (HOTSPOT)</td><td colspan="4">No Bulk Coolant Boiling
No burnout in local hotspots</td></tr>
</table>

4.4 PHENOMENA INFLUENCING CLAD AND WRAPPER

The following are the phenomena and the parameters that influence clad and wrapper design and performance.

- Swelling
- Irradiation creep
- Temperature gradients
- Thermal shocks
- Handling load
- Bowing
- Dilation
- Contact forces
- Coolant pressure
- Fission gas pressure
- Fuel clad mechanical interaction pressure
- Sodium corrosion
- Fuel clad chemical interaction

In particular, the phenomena that affect the fuel pin design are depicted in Fig. 4.2 below.

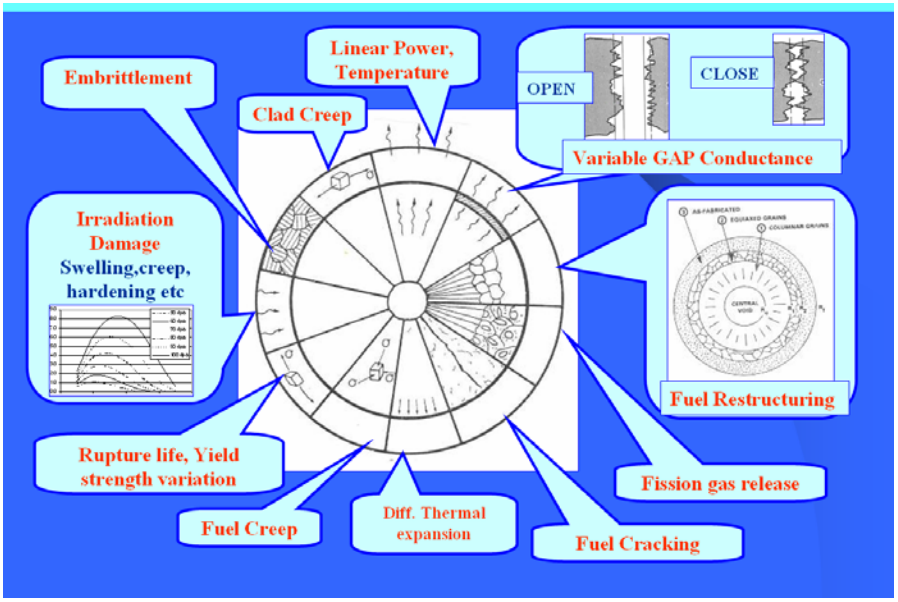

Fig. 4.2 : Phenomena affecting fuel pin design

4.5 STRESS ANALYSIS

The various stresses that act on the clad tube are listed below:

(i) Stresses due to pressure loading

(ii) Discontinuity stresses at the plug-tube joint

(iii) Stresses due to radial temperature gradient

(iv) Stresses due to temperature and swelling gradients in the axial direction

(v) Stresses due to thermal shocks

(vi) Clad wastage due to chemical interaction between clad and fuel pellets

The stresses that arise and simple analytical correlations that can be used for calculating the stresses are briefly described below. Dedicated computer codes for fuel performance analysis or the standard computer codes can be used for working out the stresses. Nevertheless, simple correlations can be used to get an idea of the stresses and to arrive at the preliminary dimensional parameters before embarking on a detailed analysis for fine tuning the dimensions. Simple equations are given here to give an insight into the kind of parameters involved in the stress analysis. The stresses will be suiably combined and used to find out the margin to creep rupture for a given CDF.

4.5.1 Stresses due to pressure loading

The tangential and axial stresses induced in the tube wall due to internal pressure are given by

$$\sigma_{pt} = \frac{PD_m}{2t}$$

$$\sigma_{pa} = \frac{PD_m}{4t}$$

Here D_m is the mean diameter of the clad tube and t is the clad thickness. In these expressions, both pressure P and t are functions of time. The thickness of the tube is decreased due to corrosion both by hot sodium and fission products.

Finding the pressure

Pressure stress is a function of

- Amount of gas formed in the fuel
- Amount of gas released from the fuel
- Temperature of gas and
- Volume of fission gas plenum.

Fission gas Generation & Release

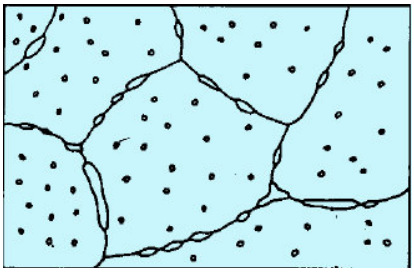

Fig. 4.3 : Distribution of fission gas in fuel matrix

Fission gas is produced during the fission process either directly from fission or from decay of the fission products (Fig. 4.3). For a fast reactor, about 0.27 is fission yield in the form of stable fission gas. i.e., for every fission process, which generates fission products out of which 27% yield as stable fission product. Xenon consists the maximum portion of the fission gas followed by krypton. The process of nucleation of fission gas bubble its growth & diffusion is a very complex. The fission gas thus generated is either retained in the fuel matrix or released to the plenum through cracks. The portion retained in the matrix causes swelling of the fuel and the escaped fission gas pressurizes the plenum.

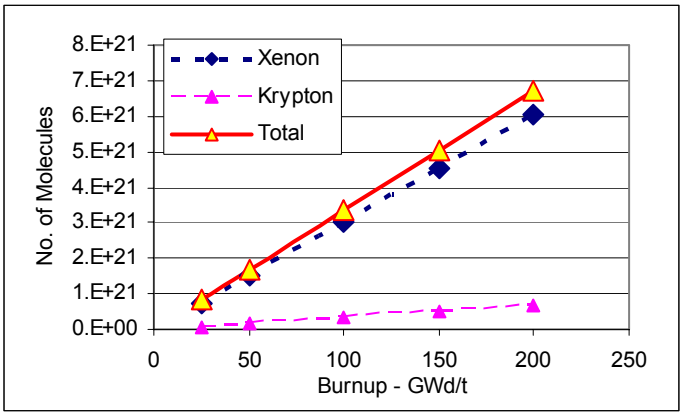

Fig. 4.4 : Fission Gas generated as a function of burnup

The release of fission gas is proportional to temperature. Up to 1300K, there is no significant fission gas release there after, it increases and especially above 1900K, significant portions are released to fission gas plenum. So most of the fission gas produced in the periphery of the pellet is retained due to its low temperature which is a concern in case of fuel transients which may lead to sudden release of the fission gas.

Fig 4.4 shows the variation of fission gas pressure in the pin from BOL to EOL. Fig. 4.5 shows the fission gas release in case of oxide fuels.

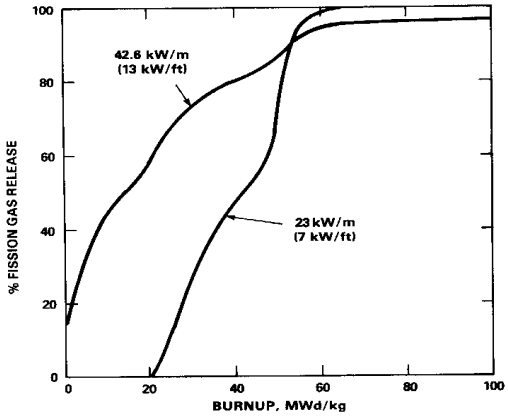

Fig. 4.5 : Percentage of gas release as a function of burnup in Oxide fuel

Fission gas release and plenum length

A common technique for calculating the plenum pressure is to calculate the volume Vo, of the fission gas at a STP temperature T_o = 273 K and pressure P_o = 1 atm = 1.013×10^5 pa.

As per gas equation, $$\frac{P_p V_p}{T_p} = \frac{P_o V_o}{T_o}$$

Let α_o = vol. of fission gas released per cubic meter of fuel at STP.
We can express $V_o = \alpha_o V_f$

$$\therefore \frac{P_p V_p}{T_p} = \alpha_o \frac{V_f P_o}{273}$$

Since gas plenum is contained in the same cladding

$$\therefore \frac{V_p}{V_f} = \frac{L_p}{L_f}$$

$\therefore P_p L_p = \alpha_o L_f \frac{T_p . P_o}{273}$

α_o is related to fission gas release fraction (F) and burnup (B)

$$\therefore \alpha_o = \frac{FnRT_o}{P_o}$$

Where, n - kg-mol fission gas produced / m^3 fuel

R- Universal gas constant 8317 J/Kg.mol.K

Now for an oxide fuel pin with a density of ~11000 kg/m^3, a smear density of 85% & a fission gas yield of 27%; n can be calculated as follows:

$$n = B \frac{MWd}{kg.heavyMet.} \frac{2.93x10^{16} \frac{fissions}{MWs} 86400 \frac{s}{d}}{6.023x10^{26} \frac{molecules}{kg.Mol}}$$

$$X \quad 11000x0.85 \frac{kg.Oxidex}{m^3 Fuel} \frac{238}{270} \frac{kg.Heavymetal}{kg.Oxide}$$

$$X \quad 0.27 \frac{kg.Mol.fissiongas}{kg.Mol.Fissioned} = 0.94x10^{-2} B$$

Now $\alpha_o = \frac{0.94x10^{-2} x8317x273}{1.013x10^5} FB$

From this the fission gas pressure may be evaluated. Pressure increases with burn-up and hence the stresses induced in the clad tube.

Hoop stress in the clad tube is given by,

$\sigma_p = p\ d / (2t)$

4.5.2 Discontinuity stresses at the plug-tube joint

The discontinuity moment and shear forces are calculated assuming the plug to be infinitely rigid.

Mo - $p / 2\beta^2$

Qo - p / β

Here, P is the internal pressure and β is a constant for the tube equal to

$$\sqrt[4]{\frac{3\left(1-\upsilon^2\right)}{a^2.t^2}}$$

a = mean diameter of the tube

t = thickness of the wall of the tube ; Poisson's ratio, υ = 0.3

The stress distribution in the vicinity of the discontinuity is found out knowing Mo, Qo, the normal force in the circumferential direction which is a function of Mo and Qo and the moment Mo in the circumferential direction.

4.5.3 Stresses due to radial temperature gradient

For a logarithmic temperature gradient across the wall, when the thickness of the wall is small enough in comparison with the inside radius to neglect the second order, the stresses are given by the following expressions.

$$\sigma_\theta = \sigma_Z = \frac{\alpha.E.\Delta T.\left(1\pm\frac{m}{3}\right).}{2(1-\upsilon)}$$ at the inner & outer wall

where $\sigma_\theta \; and \sigma_Z$ represent the circumferential and axial stresses respectively, m is the ratio of wall thickness to the inner radius and ΔT is the temperature drop in the tube wall given by

$$\Delta T = \frac{H}{2\pi.Kc}.\ln\frac{Do}{Di}$$

Here H is the linear heat rating of the fuel in W/cm (varies along the column), Kc is the thermal conductivity of the clad material and Do and Di are outside and inside diameters of the tube respectively.

4.5.4 Stresses due to temperature and swelling gradients in the axial direction

The temperature and swelling gradients vary along the length of the cladding tube. Hence, the length can be divided into a number of segments for which the calculations are carried out. The nature of the gradient is taken into account while calculating the discontinuity moments which decided the sign.

The discontinuity moment at a point where the scope changes is given by

$$Mo = \frac{\beta.D.R_{mean}}{2}.\frac{\Delta E}{\Delta X_1}+\frac{\Delta E}{\Delta X_2}$$

with appropriate signs for $\frac{\Delta E}{\Delta X}$

In the case of temperature gradients, $\frac{\Delta E}{\Delta X}$ is given by $\alpha \; . \; \frac{\Delta T}{\Delta X}$,

where α is the coefficient of linear thermal expansion, β is the constant for the tube (as given in 4.5.2), R_{mean} is the mean radius of the clad tube and D is given by the expression given below.

$$D = E.t^3 / [12 (1 - \upsilon^2)]$$

Once the moment is calculated, stresses can be calculated following the classical equations available.

4.5.5 Stresses due to thermal shocks

Fuel pin is subjected to thermal shocks during transients, both cold and hot shocks. Due to these shocks, stresses will be induced which have to be considered in the analysis. When the diameter to thickness ratio is sufficiently large, the stresses can be calculated using the formulas applicable for plane walls which is given below.

$$\sigma = \frac{E.\alpha.\Delta T}{(1-\upsilon)}.F$$

Where F is a factor $\leq$ 1, depending on the Fourier number F_0 and other parameters explained below. F_0 is defined as follows. The factor F will be used according to the Fourier number.

$$F_0 = \frac{\delta \tau}{(t^2)}.$$

δ - thermal diffusivity of clad material cm^2/s
t - thickness, cm
τ - duration of the shock, s

By this approach, the maximum stress will be obtained at the side of the clad tube where the shock occurs. The stress will be tensile in nature in the case of cold shock and compressive in the case of hot shock. Normally, stresses due to shocks will be small compared to fission gas pressure since the tube is thinner.

4.5.6 Clad wastage due to chemical interaction of clad and fuel pellets

Due to interaction with fuel on one side and with coolant on the other side, the thickness of the clad gradually decreases. The reduction in thickness is a very important aspect for designer as it increases the stresses in the clad. The wastage is mainly due to chemical interaction between clad and the fission products of the fuel. The following correlations give the wastage of clad from fuel side as a function of burnup which have to be evolved as a function of fuel parameters and the design conditions.

$d=(0.507*(O/M-1.935)*B*(T-705)+20.5)*F$ μm when O/M<1.98

$d=((O/M-1.94)*B*(T-800)^{0.5}*LHR^{0.5})*F$ μm when O/M>1.98

where,

d - Depth of penetration in clad, μm
B - Burnup in at%
O/M - As fabricated O/M ratio
T - Local time averaged cladding inner surface temperature. K
LHR - Linear heat rating
F - factor as a function of O/M & Pu fraction.

The loss due to coolant clad interaction is much lower compared to fuel clad interaction. In the case of sodium as coolant, again correlations derived from experiments will normally be used. Sometimes, the maximum wastage at the end of life is taken conservatively since the quantity is small with high sodium purity. The following fig. 4.6 show the loss in clad thickness due to fuel and sodium corrosion (taken as 4 μm per year) for a typical fast reactor fuel pin case.

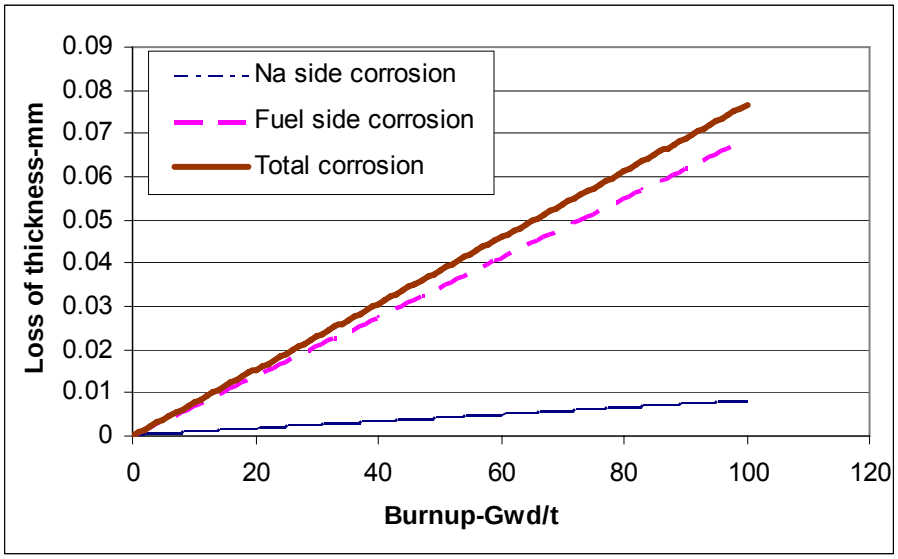

Fig. 4.6. Clad wastage as a function of burnup

4.6 FLOW INDUCED VIBRATION OF FUEL PIN

4.6.1 Background

Fast reactor fuel pins are slender structures in general. Fuel pins are vertically held in the form of a bundle within a hexagonal wrapper tube. The pins are separated by spacer wires wound around the pins helically which has been adopted in many fast reactors.

The coolant flow is in the turbulence regime and it induces vibrations in a subassembly which consists of two things; fuel pin vibration and the overall subassembly vibration.

Flow induced vibration (FIV) of a fuel pin is an important subject which needs attention since this had been a major concern. These vibrations cause damage to the clad tubes through fretting, wear and fatigue. Stresses will also be induced due to bending. Hence, the stresses have to be within the limits when checked together with other contributions. Also, the fretting and wear dictate the spacing between the pins which is also influenced by hydraulic and neutronic considerations.

4.6.2 Analytical prediction of pin vibration

The pin vibration due to flow could be modelled by computer codes in a detailed way. Nevertheless, empirical correlations based on experiments have been widely used to get the first hand values which then could be verified through experiments. In literature, several empirical correlations are available. In order to get insight into the parameters which influence the FIV, Burgreen's correlation is given below.

$$\left(\delta / D_h\right)^{1.3} = 0.83 x 10^{-10} . K_1 . \Pi \ 1/2 . \Omega$$

δ	=	vibration amplitude (peak to peak) in mm
D_h	=	hydraulic diameter of pin
K_1	=	end fixity coefficient, depends on pin end fixing conditions
Π	=	$\rho_{Na} . V^2 . L^4 / EI$
P_{Na}	=	density of sodium, kg/m^3
V	=	velocity of sodium in the bundle, m / sec
L	=	span length, m (axial unsupported length between two pitch)
E	=	Young's modulus of clad material, N/m^2
I	=	Moment of Inertia of pin, m ^{4}
Ω	=	$P_{Na} . V^2 / \mu . \omega_n$
μ	=	viscosity of sodium, NS/m^2
ω_n	=	$2 \pi f_n$
f_n	=	natural frequency of vibration of pin

The other data required are clad dimensions and material properties. In order to give an insight into the magnitude of the quantities associated with FIV, the results of PFBR fuel pin are given in tables

Using the above correlation and data, the pin vibration amplitude are estimated for PFBR fuel pin and the corresponding bending stress and strain are also computed and is shown in Tables 4.4 through 4.7.

Table 4.4 : Permissible vibration disp. & strain from fretting and wear considerations (spacer wire pitch = 150 mm)

Span length (mm)	Disp (*) (mm)	Bending stress (max) MPa	Strain (max)
25.0	5 x 10^{-3}	40.0	2.5 x 10^{-4}
37.7	5 x 10^{-3}	18.0	1.13 x 10^{-4}
50.0	5 x 10^{-3}	10.0	0.625 x 10^{-4}
150.0	5 x 10^{-3}	1.12	0.07 x 10^{-4}

Table 4.5: Permissible vibration disp. & strain from fatigue considerations

Span length (mm)	Disp (*) (mm)	Bending stress (max) MPa	Strain (max)
25.0	1.85 x 10^{-3}	15.0	0.94 x 10^{-4}
37.7	4.16 x 10^{-3}	15.0	0.94 x 10^{-4}
50.0	7.4 x 10^{-3}	15.0	0.94 x 10^{-4}
150.0	66.6 x 10^{-3}	15.0	0.94 x 10^{-4}

Table 4.6: Natural frequencies of fuel pin

Spacer wire pitch (mm)	Span (mm)	Natural frequency (Hz)
150	25.0	10490
	37.5	4663
	50.0	2623
	150.0	291
200	33.3	5902
	50.0	2623
	66.7	1474
	200.0	164
250	41.7	3771
	62.5	1679
	83.3	944
	250.0	105

Table 4.7: Analytical estimation of PFBR fuel pin vibration

Spacer wire pitch (mm)	Span length (mm)	Disp x 10^{-3} (mm)	Bending stress (MPa)	Strain x 10^{-6}	Permissible vibration disp	
					Fretting & wear x 10^{-3} (mm)	Fatigue x 10^{-3} (mm)
150	25.0	0.007	0.06	0.347	5.0	1.85
	37.0	0.024	0.09	0.538	5.0	4.16
	50.0	0.058	0.12	0.728	5.0	7.40
	150.0	1.689	0.38	2.378	5.0	66.60
200	33.3	0.017	0.08	0.470	5.0	3.29
	50.0	0.058	0.12	0.728	5.0	7.40
	66.7	0.140	0.16	0.995	5.0	13.2
	200.0	4.093	0.52	3.240	5.0	118.4
250	41.7	0.033	0.10	0.600	5.0	5.15
	62.5	0.114	0.15	0.925	5.0	11.6
	83.3	0.277	0.20	1.265	5.0	20.5
	250.0	8.133	0.66	4.120	5.0	185.0

* disp. Refers to ½ peak to peak amplitude;
* stress and strain are maximum quantities

4.7 SUBASSEMBLY DESIGN

Subassembly (SA) refers to the cluster of fuel pins that are grouped together as a single unit. It is already seen as to how the fuel pin diameter is selected. The fuel pin structural design also has been covered in the previous section. Almost about 90% of te power is produced in the active core. Hence, the basis by which a number of pins are grouped together and the influence of geometry and material assume importance in the subassembly design. The other subassemblies like blanket, reflector and shielding subassemblies are designed by the same approach that is adopted for fuel SA.

4.7.1 Wrapper tube

The wrapper tube around the fuel pin cluster is needed to accomplish the following.

- Wrapper tube facilitates the coolant flow past the fuel pins so that cooling is facilitated.

- It allows individual assembly orificing (flow zoning) which helps in achieving the power to flow ratio as desired to the extent possible.
- It provides structural support for the pin bundle.
- It provides a mechanical means to load the pins into core.
- It provides a barrier to potential propagation of a possible accident initiated by rupture of a few pins to rest of the core.

The design of the wrapper tube involves its sizing and the thickness mainly. Sizing depend on the number of pins that are grouped together within a wrapper tube. The thickness depends on the load the wrapper is subjected to and the coolant pressure inside the wrapper and the thermal and swelling gradients similar to fuel pin clad. The thickness has two conflicting requirements. Neutronic considerations demand less thikness and the structural and fabrication consideration would need higher thickness. In addition, the wrapper is subjected to irradiation induced phenomena such as bowing and lateral dilatation which are covered later in this lecture. The spacing between the SA also depends on the dilation having large influence in neutronics in terms of optimum volume fractions.

4.7.2 Basis for Number of pins in a fuel SA

The number of pins that can be grouped together within a wrapper depends on the following parameters.

- Reactivity worth of a SA is to be limited to avoid large reactivity swing during refuelling.
- Decay heat level is to be optimum. Too large decay heat would make handling difficult.
- Assembly weight (considering handling) is to be minimum.
- Mechanical performance
  - Large sheath results in more stress and deformation due to coolant pressure.
  - bowing and dilation problems become magnified with larger size SA.
- Cost reduces by reducing number of SAs; i.e., by increasing no. of pins per SA.
- Criticality during shipment. SA should remain sub-critical even when flooded with water.
- Burnup (Average burnup goes down for a given peak burnup, due to more power gradient in larger SA).
- Refuelling time: Larger assemblies require few steps, hence less time.

  Usually 217 or 271 pins are chosen for power reactors; i.e., 8 or 10 rows of fuel pins.

4.7.3 Pin spacers

For spacing the pins within the wrapper, to facilitate proper coolant flow around the pins, two concepts are considered; helically wound spacer wire around all pins or use of grid spacers in the form of honey comb structure. Their advantages and disadvantages are given below briefly.

Helical wire

It facilitates easy and inexpensive fabrication. The flow induced vibration would be less as the pins are tightly held. Mixing of the coolant is enhanced due to cross flow facilitated by spacer wire. However, the pressure drop across the pin bundle would be more.

Spacer grids

Honey comb type spacer grids are stacked at suitable axial levels. This gives the advantage of occupying less steel volume within the core which is advantageous

neutronically. Pressure drop would be less compared to spacer wires. However, the manufacture places a heavy demand in terms of very tight control on the tolerances. The major disadvantage is that it is prone to coolant flow blockage by way of accumulation of fuel debris or external debris at grids.

Wire wrap concept has been adopted in almost all the fast reactors.

4.7.4 Fission Gas Plenum

Fission gas plenum is provided within the fuel pin to accommodate the fission gas generated. It can be placed either below or above the active core or in both locations. In US designs (FFTF & CRBRP), plenum is above core, whereas in French (Phenix, SPX) and Indian PFBR design, small upper & large lower plenum are provided. Usually, plenum below core is preferred if the burnup is larger. And it will be about 70-95 % of the active core height.

Plenum above core has the advantage that clad rupture in the plenum region would not allow fission gas to pass through the core. However, the disadvantages are (i) Coolant is at its higher temperature above the core and the plenum length or volume to accommodate the fission gas pressure is larger than that would see the case for a plenum below the core and (ii) Longer plenum adds to the total length of fuel pin, high-pressure drop across the SA, higher pumping power and large reactor vessel.

4.7.5 Volume Fraction

Decreasing core size with a given amount of fertile plus fissile fuel leads to an increase in fissile fraction and lower fissile inventory. A triangular lattice arrangement intrinsically allows a higher fuel volume fraction than a square lattice. Higher fuel volume fraction minimises fissile loading, mainly by reducing neutron leakage. Hence, hexagonal geometry is preferred for the duct.

4.7.6 Fuel Assembly Length

Fuel subassembly length is decided by the active core length, axial shielding requirements, length of mixing zone required, length of axial blankets and the length of the fission gas plenum. It has influence on the pressure drop, coolant temperature rise and sodium void worth.

4.8 CORE RESTRAINT SYSTEM

Fast reactor core components operate under hostile and demanding environment of high neutron flux and elevated temperatures. Successful operation of of them is largely dependent on the performance of core structural materials, i.e. clad and wrapper materials of the subassembly, which are subjected to intense neutron irradiation. Due to the high fluence on the materials, undesirable effects such as swelling, creep, embrittlement etc. will occur. The effect of material irradiation manifest in the form two types of deformation in the SA. They are SA bowing and wrapper dilation.

Neutron flux and temperature across a SA will be different as they have a radial power profile and radial flux distribution. Due to this, there would be

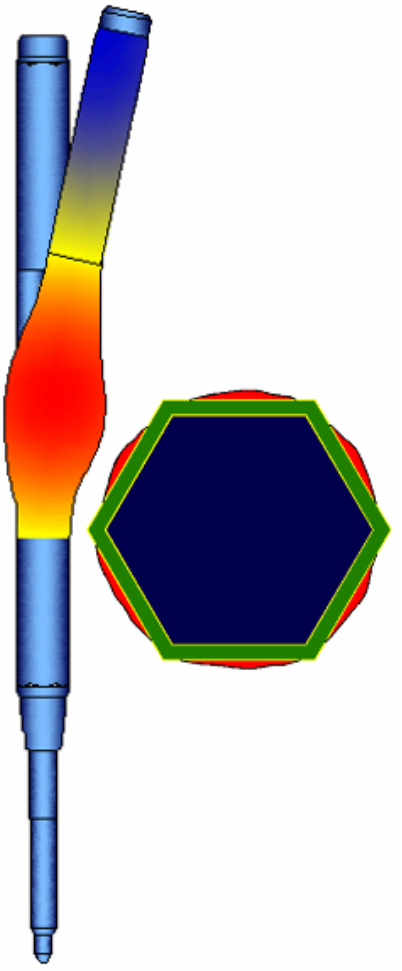

Fig. 4.7: SA bowing and dilation

differential thermal expansion and differential swelling across the width of the SA. Hence, the SA will tend to bow to accommodate the differential expansion. Higher the gradient, higher will be the bowing. The extent of bowing is dependant on its location in the core as the flux tends to become less towards the core periphery. A typical bowed SA is shown in Fig. 4.7.

Coolant is flowing through the SA at a given pressure. Since the neutron flux is likely to be maximum at the core middle level, the wrapper tends to increase in size due to thermal expansion and swelling. Also, since the wrapper is subjected to coolant pressure induced stresses and it is at high temperature, the wrapper tube will experience thermal creep and irradiation creep. The combined action of swelling and irradiation creep manifest in the form of increase in the lateral dimension of the hexagonal shape which is called dilatation or dilation (fig 4.7). Obviously, the SA dilation will be high at or near the middle column of the active core height. At higher burnup, the dilation may cause even closure of the inter SA gap and hence the adjacent SA may touch each other exerting pressure on one another. Due to this, there would be additional frictional force which has to be overcome by the fuel handling machines while unloading the SA from the core. Overcoming this problem will require higher inter SA gap which will affect the neutronic volume frcations.

The phenomena of bowing has acquired importance due to its effects on reactivity change within the core and deformation and interaction forces on the subassemblies which is of concern to safety and control and also to the design of the fuel handling machines.

In order to provide design solutions to the bowing, core restraint system is needed and designed accordingly. The core restraint system allows for core SA interaction so that the resulting deformation are as per the intended design limits. The restraint system should provide for accommodating the bowing deformation and at the same time should be capable of resulting in moderate deformations and the contact forces and with minimum reactivity changes.

Requirements of core restraint system

1. The SA deformation should be within the limits and reach of fuel SA handling machines
2. The SA deformation should not affect the core outlet temperature monitoring which forms a safety instrumentation system.
3. The resulting contact forces should be within the handling machines capacity
4. Should not result in high reactivity change
5. It should be able to accommodate the SA dilation.

The core restraint system design effects the parameters like, number of contact pads, location of pads, pad size and pad thickness or in other words inter-pad gap. It is also important to estimate the contact forces between the subassemblies and the friction force in sodium medium to evaluate the forces required for loading/unloading of the fuel subassemblies during fuel handling operation.

4.8.1 Design Criteria

The design criteria for the core restraint system is as follows :

a) deformation of the components

- minimum core subassembly head displacement

- minimum In-core subassembly bending

b) forces on the following components should be within the limits

- pads

- SA foot and the grid plate sleeve

- Handling mechanisms

c) reactivity effects

The allowed values differ from one reactor to the other, corresponding to the design of the subassemblies, the handling device and the reactivity change limit considerations.

4.8.2 Types of systems

There are basically three types restraint system concepts that can be adopted in the design.

(i) Active Restraint

External restraints are provided around the core in the form of yokes which provided lateral loads on the SA according to the conditions needed. This has the advantages of limiting the variables at the desire of the designer. But the design of the system would be complex requiring sophisticated mechanisms that should operate in sodium.

(ii) Passive Restraint

In this concept, thick rings or shells are placed surrounding the core and blanket SA which will limit the deformation to a particular design value as dictated by the restraint system rigidity. In this concept, the deformations can be limited to a large extent but the contact forces would be very high. Beyond a certain burnup and the consequent contact forces, the SA may tend to bow inward at the active core level, of course which depends on the pad system design.

(iii) Natural Restraint

SA is supported vertically as a cantilever on the grid plate and contact pads are provided on the faces of the SA. The SA are allowed to bow freely until the contact is made with shield SA at the core periphery. Thus, the restraint is given by the surrounding reflector and/or shielding SA which also absorb some deflections. This type of system would result in moderate deflections and contact forces and consequent reactivity changes. Due to low maintenance problem passive systems are preferred over the active systems. Typical passive support system is shown in Fig. 4.8.

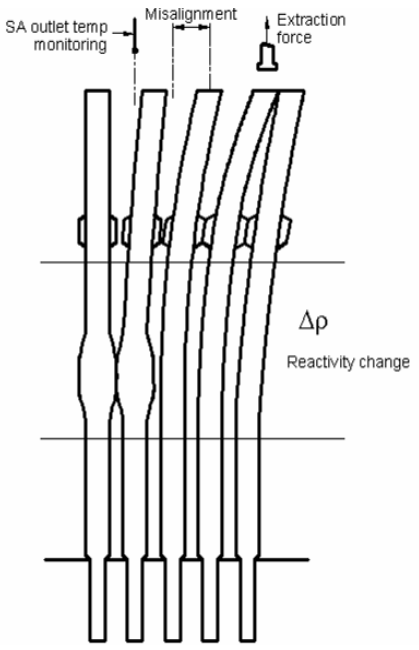

Fig. 4.8 : Natural restraint system

4.8.3 Typical results for natural core restraint system

The typical results of natural core restraint system adopted for a power reactor (PFBR) are shown in Fig. 4.9 through Fig. 4.11. The results are for a peak burnup of 100 GWd/t burnup with 20% CW D9 as the wrapper material and the coolant inlet temperature and the temperature rise are approx 400 ^{o}C and 150 ^{o}C. The results are given for a 60 ^{o} sector of a core which is symmetric.

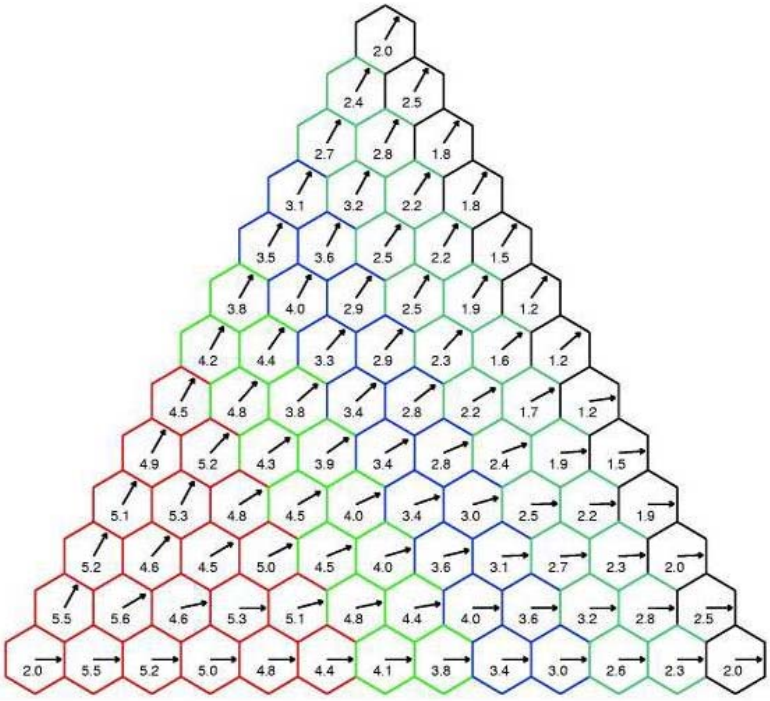

Fig. 4.9 : Resultant deflection of SA after 100 GWd/t burnup in shutdown condition at pad location

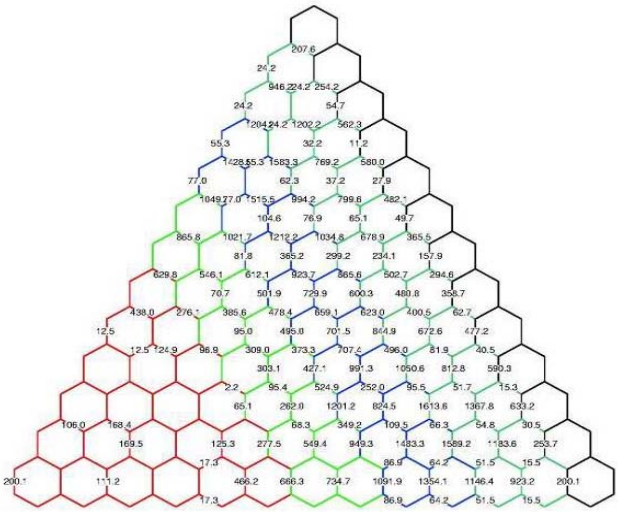

Fig. 4.10 : Reactive forces between the SA after 100 GWd/t burnup in shutdown condition at pad locations

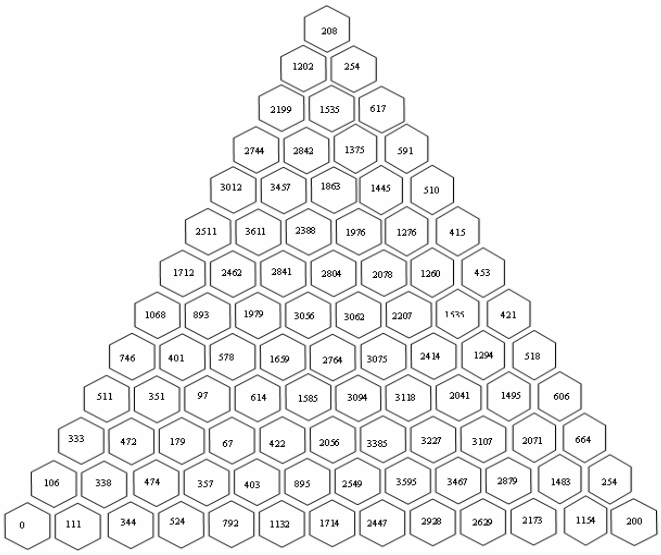

Fig. 4.11 : Addl extraction forces reqd excluding SA weight with a suitable friction factor for contact forces after 100 GWd/t burnup in shutdown condition

4.9 Structural Materials

The core of fast reactor consists of thin-walled fuel pins encased in a hexagonal wrapper tube constituting one fuel subassembly. Fuel pins are separated from one another to ensure adequate coolant flow by a helical spacer wire. Cladding forms the first barrier against possible dispersion of fissile material and fission products. As the neutron flux levels in fast reactors are about two orders of magnitude higher (~10^{15} n/cm^2s^{-1}) than that in thermal reactors, the core materials are subjected to a high fast neutron flux coupled with high temperatures (523-973K) resulting in high level of atomic displacements as seen earlier.

The choice of the core structural materials has been mostly guided by their resistance to irradiation induced swelling and the related dimensional changes and deterioration of their mechanical properties. The first generation materials belonged to austenitic steels of type AISI 304 and 316 SS. As these steels quickly reached their limits because of unacceptable void swelling, many improvements were made by modifications of the metallurgical structure by suitable thermo-mechanical treatments, addition of stabilising elements, changes in the chemical composition of major and minor elements etc. This led to the development of advanced core structural materials such as D9 and D9I. Another class of steels namely the ferritic-martensitic steel is being considered as the long term solution because of their very low rates of void swelling. Various issues concerning the performance of these structural materials are discussed briefly in the following sections.

4.9.1 Irradiation Behaviour of Austenitic Stainless Steels

Four major phenomena that influence the performance of these steels as core components include phase stability, void swelling, irradiation creep and changes in mechanical properties. These phenomena are intimately linked and it has been shown that void swelling depends sensitively on the evolution of phases in austenitic stainless steels and is the dominant determinant of both irradiation creep behaviour and mechanical properties. Alterations in chemical composition and microstructure which influence void swelling also exert strong effect on irradiation creep

Phase stability

During irradiation, three general classes of phases can form in type 316 SS and its variants. The first class is radiation-enhanced or radiation retarded thermal phases. In this group, precipitate phases form due to thermal aging which includes M_6C, $M_{23}C_6$ and MC carbides, σ and χ intermetallics. The second class is radiation-modified phases which are different from the composition found during thermal aging. These are primarily M_6C, Laves and FeTiP. The third class is radiation-induced phases which are uniquely produced by reactor irradiation and the phases in this category include Ni_3Si (γ') and G-phase ($M_6Ni_{16}Si_7$) silicides and needle-shaped MP, M_3P or M_2P phosphides.

Radiation-induced segregation occurs due to the presence of a large supersaturation of vacancies and interstitials. The mechanisms of radiation induced segregation are solute drag effect and inverse Kirkendall effect. The various precipitates formed due to segregation involving elements like Ni & Si is intimately linked to the onset of void swelling.

Void Swelling

Voids form in austenitic stainless steels in the temperature range 673-973K under neutron irradiation in FBRs. This result from the agglomeration of vacancies produced due to atomic displacements. Helium produced from (n,α) reactions stabilizes the voids. The formation and growth of voids is sensitive to nearly all metallurgical variables like chemical composition and thermo-mechanical history and irradiation parameters like fluence, dose

rate and irradiation temperature. The fluence dependence of swelling can be described as a low swelling transient period followed by an acceleration to a regime of near linear swelling (Fig.4.12). Metallurgical parameters are found to be sensitive only in the duration of incubation and transient regimes. The steady state swelling regime is relatively insensitive to these variables with the swelling rate of most austenitic alloys being ≈1% per dpa over a wide range of irradiation temperatures.

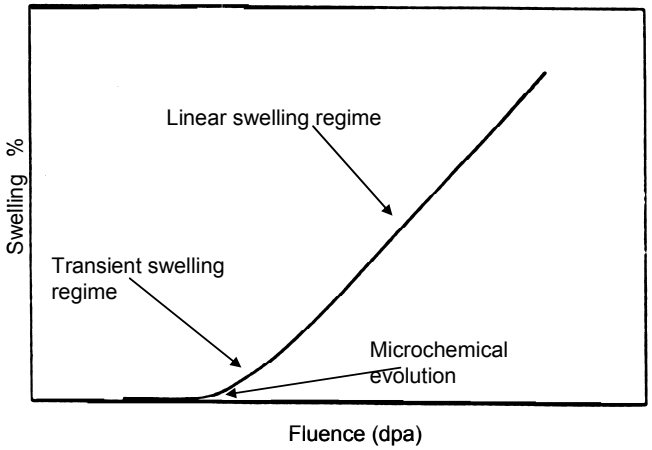

Fig. 4.12 : Typical structural material swelling behaviour

The trend in development of radiation resistant 300 series austenitic stainless steels has been to increase nickel content and decrease chromium concentration in comparison to standard versions. The presence of nickel in solution is suggested to enhance effective vacancy diffusion coefficient and therefore leads to reduced void nucleation rate. Increasing nickel and reducing chromium would increase stability of the γ phase against precipitation of undesirable phases that also remove certain solutes responsible for conferring void swelling resistance to these steels.

It has been found that certain solutes like titanium, silicon, phosphorous, niobium, boron and carbon play a dominant role in improving void swelling resistance by extending the duration of the transient regime. The presence of fine carbides of Ti and Nb provides recombination sites for point defects and hence reduces their supersaturation and consequently void swelling. Ti/C ratio has been shown to play an important role in determining irradiation behavior of austenitic steels. Maximum swelling resistance has been obtained when Ti/C ratio is below the stoichiometric composition i.e. when the material is understabilized.

Silicon improves void swelling resistance of austenitic stainless steels through its role as a fast diffusing species which reduces supersaturation of vacancies by their relatively fast migration to sinks. Similarly the improvement in swelling resistance by phosphorous additions arises due to a decrease in void density caused by uniform distribution of needle-shaped phosphides.

The degree of cold work which influences dislocation density is an important parameter determining the void swelling behavior of austenitic stainless steels. Since dislocations act as sinks for point defects, their density influences void swelling. Cold work also influences swelling behavior by providing sites for nucleation of precipitates as well as for trapping of helium bubbles. The cold work is also specified with a view to enhancing creep strength.

Irradiation Creep

Irradiation creep is caused due to the combined effects of an external non-hydrostatic stresses and presence of both interstitial atoms and vacancies at very large supersaturation levels. The main characteristic of irradiation creep is that it occurs at relatively low temperatures where the thermal creep is negligibly small. Stress-induced preferential absorption (SIPA) of interstitials at dislocations is considered as the dominant mechanism of irradiation creep. The process SIPA leads to creep deformation, which is proportional to the applied stress and the irradiation dose. Thermal creep can also be altered due to microstructural changes as a result of irradiation.

There is ample evidence to show that in most of the austenitic stainless steels, there is a direct coupling between the creep and swelling rates after swelling begins. An important consequence of this coupling is that swelling resistant materials are also resistant to irradiation creep. In fact, solutes such as phosphorus which reduce swelling also reduce creep strain in austenitic stainless steels. Similar to its influence on void swelling, nickel content in austenitic stainless steels has also been seen to decrease creep strain.

Irradiation-induced Embrittlement

Fast neutron irradiation strongly affects the mechanical properties of austenitic stainless steel alloys especially the ductility. The degradation of mechanical properties, especially the loss in ductility is dependent on temperature of irradiation, prior microstructural condition and neutron fluence (dpa). Temperature is a very important variable as it determines the stability, distribution and morphology of the defect structures such as dislocation loops, network dislocations, voids and helium bubbles.

There are three temperature regimes of importance to embrittlement: A low temperature regime where void swelling is not significant, an intermediate temperature regime where swelling is predominant and a high temperature regime where the mobility of helium is sufficient to cause intergranular failures. In the low temperature regime, for annealed austenitic stainless steels there is an increase in yield strength and ultimate tensile strength and a reduction in ductility. The increase in yield strength is much more pronounced compared to the increase in ultimate tensile strength. This reduced capacity of the material to work harden leads to reduced ductility. There is a change in the fracture mode from ductile tearing in the unirradiated material to transgranular channel fracture after irradiation.

The ductility parameters recover significantly at intermediate temperatures before decreasing again above ~ 873K. The reduced ductility at high temperatures is associated with an increased tendency for fracture to occur along the grain boundaries. This has been attributed to the phenomenon of helium embrittlement. At temperatures and doses where void swelling is significant, it exerts strong influence on mechanical properties. This correlation between ductility and swelling could be attributed to either the direct effect of voidage in promoting brittle fracture or to the indirect effect of radiation induced segregation due to presence of voids. Radiation induced segregation could lead to instability of austenitic matrix due to nickel segregation at void surfaces facilitating transformation to martensite which would induce embrittlement. Thus the measures to improve swelling resistance of austenitic stainless steels would also enhance resistance to embrittlement.

Engineering Consequences of Irradiation Effects

Engineering consequences of irradiation-induced changes such as void swelling, irradiation creep and embrittlement determine the residence time of core components and hence limit the achievable burn up. Deformations of various components of the subassemblies can occur due to void swelling, thermal creep and irradiation creep. Swelling and irradiation creep are very sensitive to environmental variables, temporal and spatial gradients which exist throughout the core. Limits have to be specified on deformations in order to avoid interactions between the core components. The latter aspect is very important to permit insertion and removal of core components during refuelling using only moderate loads.

Differential swelling can occur because of gradients in flux and temperature at different locations in the core. Non-uniform deformations due to differential swelling of pin and spacer wire should be limited. If the spacer wire deformation is higher than the pin deformation, the sodium coolant flow can be reduced and consequently the fuel pins overheat slightly. On the other hand, when the pin deformation is higher than that of the

spacer wire, there is a mechanical interaction and the fuel pin undergoes a helical deformation. If both fuel pin and spacer wire swell excessively, there would be interactions between the pins as well as between the fuel pins and the wrapper. Wrapper deformation should be limited; otherwise interactions between wrappers would lead to excessive loads for fuel handling. Irradiation induced void swelling and creep can produce different types of wrapper deformation. At the centre of the core, subassemblies are expected to remain straight with an elongation and an increase of distance across flats. But at the periphery, subassemblies may bow outwards due to differential void swelling on the opposite faces of the wrappers as a consequence of the neutron flux gradient. The combination of void swelling and creep induced by internal sodium pressure produces dilation and rounding of wrapper faces.

Gradients in swelling and creep lead to interaction of core components that can affect the reactivity of the core, the movement of control rods, the flow of coolant and the ability to withdraw and replace components as needed. It has been noticed that irradiation creep and embrittlement are related to swelling. Thus reduction of swelling would solve most of the engineering problems arising out of irradiation effects.

4.9.2 Ferritic Steels as Core Structural Material

Improved versions of austenitic stainless steels could be used for exposures up to 140 dpa levels. 9-12% Cr ferritic-martensitic steels are considered as the long-term solution for FBR core structural materials for displacement damages beyond 150 dpa. These alloys [9Cr-1Mo (EM10), Modified 9Cr-1Mo (Gr. 91), 9Cr-2MoVNb (EM12), 12Cr-1MoVW (HT9) etc.] have excellent swelling resistance to doses even upto 200 dpa, (1% swelling reported in HT9 after irradiation at 693 K at 200 dpa). But their creep resistance decreases drastically above 823 K. Therefore, they are not suitable for clad tubes. Since these materials also have great potential for application in thermal power plants, a lot of research work is in progress to increase the creep strength of 9-12 Cr- ferritic steels. A high thermal creep strength is not a primary requirement for the wrapper material since the operating temperatures are below or at the lower end of the creep range for these materials, and the stresses are also low. A reduced creep strength is therefore acceptable. However, the increase in ductile to brittle transition temperature (DBTT) due to irradiation is a cause of concern in ferritic steels. The upper-shelf energy and shift in DBTT appear to saturate at high irradiation doses. Significant increase in toughness (i.e. low DBTT and high upper shelf energy) have been realised by (a) avoiding the formation of delta-ferrite and ensuring fully martensitic structure in 12% Cr steels by close control of nickel and chromium equivalent element concentration (delta-ferrite regions exhibit greater void formation and swelling than adjacent regions); and (b) optimising the austenitising temperature to refine the prior austenite grain size, and tempering treatments to reduce the strength of the martensite in 9-12 % Cr steels. 9Cr-1Mo grades of ferritic steels have been reported to show the lowest increase in DBTT among the various grades of ferritic-martensitic steels.

There is a great incentive in developing ferritic-martensitic steels for cladding applications at higher temperatures ~ 923K. Towards this goal, extensive efforts are underway to improve the creep strength of 9-12% Cr steels. Alloys capable of operation upto 873-893 K have already been developed and it is likely that their temperature capability could be extended for temperatures ~ 923K with further modifications. This coupled with the fact that for metallic fuels, clad temperatures would be lower; 9-12% Cr steels with improved creep strength appear attractive.

4.9.3 ODS as core Structural Material

Although ferritic-martensitic steels have excellent void swelling resistance to doses up to 200 dpa, their creep resistance decreases drastically above 823K. Oxide dispersion strengthened steels are other alternative with the potential of having the advantage of ferritic-martensitic steel but being able to push operating temperatures to 923K and beyond. Essentially, in the ODS steels, the distribution of stable Y_2O_3 oxide particles can be controlled on a nano-scale that serves as a strong block for mobile dislocations and as a sink for radiation defects at the particle-matrix interfaces. However ODS steels are credited with bamboo-like grain structure and strong deformation texture which gives rise to anisotropic mechanical properties, especially an inferior biaxial creep rupture strength. There are indications that the controlling of grain morphology by means of recrystallisation processing and development of equiaxed structure through austenite-martensite phase transformation successfully provide improved strength and ductility in the hoop direction of ODS ferritic-martensitic steels. There are other problems with the ODS steels besides anisotropy. At present, the literature is devoid of information on the production of thick-walled parts or large-diameter tubing. Fabrication processes for these materials for heavy sections still need to be established, and this means addressing the problem of joining the materials. ODS alloys are both expensive and difficult to form into tubes and other complex shapes. Therefore, much research and development will still be necessary on forming of these materials before these alloys will be ready for structural applications.

4.10 REFLECTOR AND SHIELDING SUBASSEMBLY

The reactor core is the source of heat from nuclear fission. Schematically, the core consists of the central fuel region enveloped by blanket region followed by reflector and shielding region. Reflector Subassembly serves the following purpose:

1. It reflects the neutrons back into the core and hence neutron leakage is reduced.
2. It moderates the neutrons so that it can be absorbed in shielding subassemblies which is placed next to reflector SA and hence it shields the reactor vessel.
3. It aids the core natural restraint system by resisting the bowing of fuel and blanket SA due to thermal and flux gradients.

The shielding SA acts as a radial shielding to limit the incident neutron flux on IHX to limit the secondary sodium activation and also provide neutron & gamma shielding for the reactor vessel and major components within the vessel. Normally steel is used as the reflector material and B_4C/steel is used as the shielding material. The overall configuration of the SA will be same as that of any other fuel/blanket SA. Inside the SA, it may contain either steel pins or B_4C pins or combination of both based on the requirements. The life of reflector and shielding Subassemblies are generally longer since there is not much heat generation and they operate at relatively lower temperature and flux when compared to

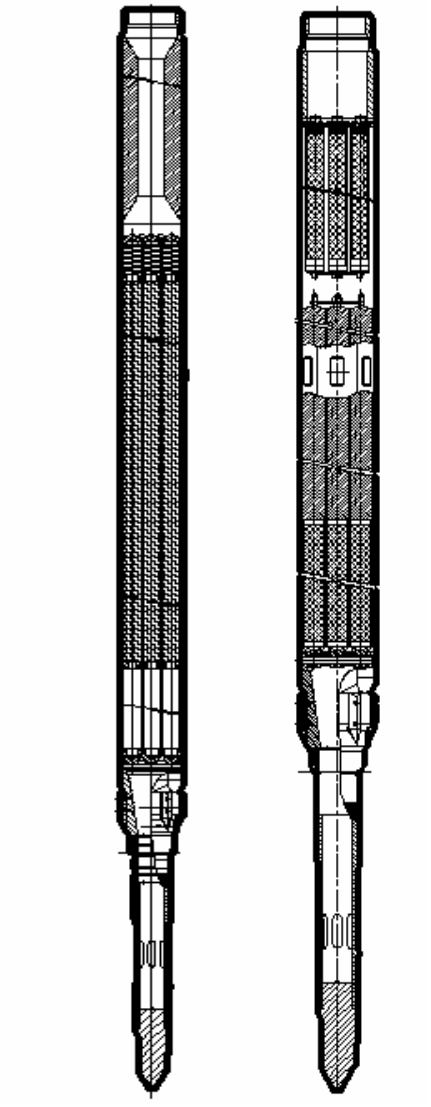

Fig. 4.13 & 4.14: REFLECTOR & SHIELDING SA

the fuel SA. A typical reflector and shielding SA used in PFBR is shown in Fig. 4.13 & 4.14 respectively.

4.11 ABSORBER / CONTROL RODS

Control rods are necessary to change the state of the reactor from one to other by manipulating the reactivity of the core. In addition, control rods ensure safety of the core in the event of emergencies, by scraming the reactor.

Functionally absorber rods could be categorised in to two types – namely safety rods and regulating/control rods. The safety rods are used to scram the reactor and the control rods are used for manipulating the reactivity of the core with accuracy.

Important parameters associated with a control rod design are total reactivity worth of control rods, number and location of control rods in the core, raising speed, lowering speed and drop time of the rods. These are decided by neutronics and safety considerations.

Preferable features of absorber material are:

- High absorption cross section
- good compatibility with cladding & coolant
- long effective life time (2 to 3 years)
- low swelling under irradiation
- high thermal conductivity
- high melting point &
- low cost.

Boron, Europium & tantalum have been given more considerations.

Boron

19 % B^{10} is present in Natural Boron. B_4C is used as absorber. In SPX1, B_4C with 93 % enriched B^{10} is used.

$_5B^{10} + _0n^1 \xrightarrow{(n, \alpha)} Li^7 + _2He^4$

$_5B^{10} + _0n^1 \longrightarrow 2\ _2He^4 + _1T^3$ (This process is only at very high energy level; i.e.,E > 1 MeV)

Since both $_3Li^7$ & $_2He^4$ atoms are larger than B^{10}, B_4C matrix swells approximately linearly with neutron exposure. The major issues with boron carbide is its swelling and the build-up of helium in the pin. Hence, large plenum must be provided or the pin has to be designed as a vented type.

Europium

In natural $_{63}Eu$, 47.8 % Eu^{151} & 52.2 % Eu^{152} are present. Averaged fast neutron cross section of Eu is twice that of B_4C.

Eu_2O_3 Euro Oxide

- absence of swelling & gas release problem due to Eu (n, γ) reaction.
- daughter nuclei of Eu (n, γ) are also good neutron absorbers and hence life of absorber rod can be extended.
- because of self-shielding effect, effective worth of Eu_2O_3 is only equivalent to that of Natural B_4C.
- low thermal conductivity

EuB_6 Euro Boride

- reactivity worth is about 10% more than Eu_2O_3; i.e., equivalent to that of 25 % B^{10} enriched B_4C.
- better thermal conductivity than Eu_2O_3.
- $_2He^4$ gas release problem is much worse than for B_4C. Hence venting out is essential.
- Being a rare earth element, supply of Europium is quite limited. Both Eu_2O_3 & EuB_6 are costly.

Tantalum

In natural $_{73}Ta$, 99.9 % Ta^{181} with trace amount of Ta^{180} is present. σ_a is about 1/3 of that of B^{10}.

$$_{73}Ta^{181} \xrightarrow{(n,\gamma)} {}_{73}Ta^{182} \xrightarrow[115\ \text{days}]{\beta-} {}_{74}W^{182} + 1.2\ \text{MeV}$$

- No gas is released
- Daughter product Ta^{182} is also a good absorber.
- Being a metal, it has a good thermal conductivity.
- Since it is not a rare element, it is not too expensive.

However, it is soluble in sodium and it has decay heat removal problem due to 115 days half-life β^- decay of Ta^{182}.

World wide, B_4C is being used as the absorber material in major reactors

The life time of absorber rods is limited by the following considerations:

1. Loss of reactivity worth of control rod due to absorber material burn-up.
2. Cladding tube integrity which might be impaired by equilibrium helium pressure inside and the swelling of B_4C pellets.
3. Dimensional variations in the control rod components due to irradiation (operational and safety considerations) such as dilation of the hexcan, bowing of the SA & swelling of foot
4. B_4C pellet cracking characteristics - At Burn-up of above 150×10^{20} captures/cm^3, it is reported that clad failure occurs due to mechanical interaction of B_4C and the clad.

References

1. Fast Breeder Reactors, Alan E. Waltar & Albert B. Reynolds, Pergamon Press 1982
2. Internal reports of IGCAR, Kalpakkam
3. “Structural design criteria for highly irradiated core components, B.C.Weli & D.V. Nelson”, Pressure Vessels and Piping : Design Technology – 1982 ; A decade of progress.
4. “Developments in elevated temperature structural design criteria, Alfred Snow & M.T. Jakub”, Ibid.
5. Fundamental aspects of nuclear reactor fuel elements, Donald R.Olander.

* * *